Interferon regulatory factor 8 regulates expression of acid ceramidase and infection susceptibility in cystic fibrosis

Aaron Ions Gardner[1], Yuqing Wu[2], Rabea Verhaegh[2], Yongjie Liu[2,3], Barbara Wilker[2], Matthias Soddemann[2], Simone Keitsch[2], Michael J. Edwards[4], Iram J. Haq[1,5], Markus Kamler[3], Katrin Anne Becker[2], Malcolm Brodlie[1,5,*,‡], and Erich Gulbins[3,4,*,‡]

From the [1]Faculty of Medical Sciences, Translational and Clinical Research Institute, Newcastle University, Newcastle upon Tyne, United Kingdom; [2]Department of Molecular Biology, [3]Department of Thoracic and Cardiovascular Surgery, University Hospital Essen, University of Duisburg-Essen, Essen, Germany; [4]Department of Surgery, University of Cincinnati College of Medicine, Cincinnati, Ohio, USA; [5]Pediatric Respiratory Medicine, Great North Children's Hospital, Newcastle upon Tyne, United Kingdom

Edited by Ursula Jakob

Most patients with cystic fibrosis (CF) suffer from acute and chronic pulmonary infections with bacterial pathogens, which often determine their life quality and expectancy. Previous studies have demonstrated a downregulation of the acid ceramidase in CF epithelial cells resulting in an increase of ceramide and a decrease of sphingosine. Sphingosine kills many bacterial pathogens, and the downregulation of sphingosine seems to determine the infection susceptibility of cystic fibrosis mice and patients. It is presently unknown how deficiency of the cystic fibrosis transmembrane conductance regulator (CFTR) connects to a marked downregulation of the acid ceramidase in human and murine CF epithelial cells. Here, we employed quantitative PCR, western blot analysis, and enzyme activity measurements to study the role of IRF8 for acid ceramidase regulation. We report that genetic deficiency or functional inhibition of CFTR/Cftr results in an upregulation of interferon regulatory factor 8 (IRF8) and a concomitant downregulation of acid ceramidase expression with CF and an increase of ceramide and a reduction of sphingosine levels in tracheal and bronchial epithelial cells from both human individuals or mice. CRISPR/Cas9- or siRNA-mediated downregulation of IRF8 prevented changes of acid ceramidase, ceramide, and sphingosine in CF epithelial cells and restored resistance to *Pseudomonas aeruginosa* infections, which is one of the most important and common pathogens in lung infection of patients with CF. These studies indicate that CFTR deficiency causes a downregulation of acid ceramidase via upregulation of IRF8, which is a central pathway to control infection susceptibility of CF cells.

Cystic fibrosis (CF) is the most common autosomal recessive disorder in the European Union (EU) and the United States (USA). On average, the disease affects one in every 2500 children born in Western countries, but some countries have an even higher incidence. CF is caused by mutations of the cystic fibrosis transmembrane conductance regulator protein (human: CFTR; mouse: Cftr) (1–3). The disease is characterized by respiratory, gastrointestinal, and reproductive complications. However, at present the gastrointestinal symptoms are usually well controlled and the pulmonary problems are the major focus of disease (3). Most patients suffer from chronic pulmonary colonization with bacterial pathogens, in particular *Pseudomonas aeruginosa* (*P. aeruginosa*) (4). A vicious cycle of infection and inflammation in the airways leads to progressive bronchiectasis. Loss of lung function is the primary cause of morbidity and mortality for these patients at present. Approximately 80% of CF patients will host *P. aeruginosa* by the age of 25 (5).

We and others have recently shown that CF epithelial cells exhibit a marked imbalance of ceramide and sphingosine (6–19). Bronchial epithelial cells from CF mice and transplant specimen exhibit increased levels of specific ceramide species and decreased levels of sphingosine. The imbalance of the two lipids in CF cells seems to be caused by a downregulation of the function and the expression of the enzyme acid ceramidase (9, 16, 19), which converts ceramide into sphingosine. We and others have previously shown that sphingosine kills many bacterial species *in vitro* and *in vivo* very efficiently, including *P. aeruginosa*, *Staphylococcus aureus* (*S. aureus*), *Staphylococcus epidermidis*, *Haemophilus influenzae*, *Escherichia coli*, *Moraxella catarrhalis*, *Burkholderia cepacia*, and *Acinetobacter baumanii* (7–9, 19–24). Sphingosine is abundantly expressed on the luminal surface of human and murine nasal, tracheal, and bronchial epithelial cells, while the levels of sphingosine are very low or almost undetectable in the corresponding epithelial cells from CF patients and CF mice (7–9, 19). We also demonstrated that inhalation of sphingosine or acid ceramidase by CF mice eliminated existing *P. aeruginosa* and *S. aureus* infections and prevented new *P. aeruginosa* or *S. aureus* infections in these mice without side effects (7–9, 19, 25). Pig experiments confirmed that inhalation of sphingosine is without adverse effects of epithelial cells of the respiratory tract (25). Collectively, these findings established a key role of sphingosine for the innate and immediate antibacterial defense in the respiratory tract.

---

‡ These two authors share senior authorship.
* For correspondence: Erich Gulbins, erich.gulbins@uni-due.de; Malcolm Brodlie, malcolm.brodlie@ncl.ac.uk.

In contrast to sphingosine, studies from several laboratories have demonstrated that ceramide levels are higher in CF epithelial cells than in normal cells (6–19). The imbalance between ceramide and sphingosine in the respiratory tract was shown to be mediated by a downregulation of the acid ceramidase protein expression correlating with a marked reduction of the activity of the acid ceramidase in tracheal and bronchial epithelial cells of mice and humans (9, 19). We have demonstrated that normalization of ceramide levels also normalizes acid ceramidase and, thereby, sphingosine levels (9). Vice versa, inhalation of acid ceramidase by CF mice or treatment of cultured human CF epithelial cells or nasal epithelial cells freshly isolated from CF patients with acid ceramidase also normalizes the increased ceramide levels in these cells (7, 9, 16, 19). This suggests that the acid ceramidase plays a key role in regulating the infection susceptibility of CF mice and possibly also humans.

Our current model suggests that deficiency of Cftr results in increased ceramide levels that mediate a downregulation of acid ceramidase and, thereby, a further upregulation of ceramide and a concomitant downregulation of sphingosine. These alterations form a vicious cycle and may cause the infection susceptibility of CF mice and human individuals with CF. At present, it is unknown how Cftr regulates acid ceramidase expression.

A link between the acid ceramidase and interferon regulatory factor 8 (IRF8), also named interferon consensus sequence binding protein, has been previously shown in chronic myelogenous leukemia cells with a marked upregulation of IRF8 and a downregulation of acid ceramidase (26). Thus, we investigated whether Cftr deficiency regulates IRF8 and, in turn, whether IRF-8 controls acid ceramidase expression in CF cells.

Here, we demonstrate that deficiency of Cftr or functional inhibition of Cftr results in upregulation of IRF8 and a concomitant downregulation of acid ceramidase protein expression and activity. Genetic downregulation of IRF8 abrogated the effect of genetic deficiency or functional inhibition of CFTR on acid ceramidase expression and activity. Genetic downregulation of IRF8 also normalized increased ceramide and reduced sphingosine levels in CF cells or after functional inhibition of CFTR. The reduced sphingosine levels upon prolonged inhibition of CFTR increased the infection susceptibility of cells to *P. aeruginosa*, which was restored by downregulation of IRF8 using siRNA technology, direct addition of sphingosine to the cells, or cellular treatment with ceramidase to generate sphingosine.

Results

To investigate whether Cftr deficiency alters expression levels of IRF8, we used CF^{MHH} mice that express low levels of Cftr, and Cftr$^{-/-}$ mice that are deficient for Cftr, but express human CFTR under the control of a fatty acid binding protein (FABP) promoter in the intestine. Both strains can be fed a normal diet. Syngenic littermates were used as controls. All mice were on a C57BL/6H background. We determined the protein expression of IRF8 in tracheal and bronchial epithelial cells from wild-type and CF mice by western blotting (Fig. 1)

and immunofluorescence staining (Fig. 2A). The results revealed a marked upregulation of IRF8 in tracheal epithelial cells from CF mice compared with the levels in wild-type mice (Fig. 1). The expression of IRF8 increased with age of the CF mice (Fig. 1). Confocal microscopy studies from trachea or lung of CF and wild-type mice confirmed the upregulation of IRF8 in epithelial cells of CF mice (Fig. 2A). IRF8 expression was normalized to actin fluorescence in epithelial cells. We also investigated whether treatment of tracheal epithelial cells with lipopolysaccharide (LPS), a paradigmatic proinflammatory mediator, results in a further change of the expression of IRF8, but failed to detect an effect of LPS on IRF8 expression (Fig. 1).

Similar to the changes in airway epithelial cells from mice trachea and bronchi, we also detected an upregulation of IRF8 in bronchial epithelial cells in histologies from explanted lungs from CF patients, who received lung transplantation, compared with the expression in bronchial epithelial cells from healthy lungs (Fig. 2B).

The relative overexpression of IRF8 in CF bronchial and tracheal epithelial cells correlated with a marked reduction of acid ceramidase activity and expression in tracheal and lung epithelial cells of CF mice as well as in bronchial epithelium from cystic fibrosis patients compared with healthy individuals (Fig. 3, A and B). Downregulation of acid ceramidase in CF cells was also age-dependent.

Further, the upregulation of IRF8 and the downregulation of acid ceramidase correlated with increased ceramide levels and a reduction of the sphingosine levels in tracheal epithelial cells from CF^{MHH} compared with the corresponding levels in wild-type mice (Fig. 3, C and D). The accumulation of ceramide and the reduction of sphingosine in tracheal epithelial cells were also age-dependent (Fig. 3, C and D).

To establish a link between the upregulation of IRF8 and the downregulation of acid ceramidase in CF cells, we treated Caco-2 epithelial cells with the pharmacological CFTR Inhibitor-172 for 2 days and determined expression of IRF8 and acid ceramidase as well as the cellular levels of ceramide and sphingosine. The results showed that treatment with the CFTR Inhibitor-172 mimicked the phenotype of Cftr deficiency with an upregulation of IRF8 mRNA (Fig. 4A) and protein expression (Fig. 4B), a downregulation of acid ceramidase activity (Fig. 4C) and mRNA (Fig. 4D) and protein expression (Fig. 4E), increased levels of ceramide (Fig. 4F), and decreased levels of sphingosine (Fig. 4G).

To investigate whether CFTR deficiency is also linked to IRF8 upregulation and acid ceramidase downregulation in human epithelial cells, we employed cultures of primary human airway epithelial cells from healthy and CF individuals. IRF8 mRNA levels were increased approximately tenfold (Fig. 5A) and IRF8 protein levels were increased threefold in CF cells compared with cells from healthy individuals (Fig. 5B). Acid ceramidase activity was markedly reduced in CF epithelial cells (Fig. 5C). We employed Lipofectamine CRISPR/Cas9 transfection to target IRF8. As we are unable to clonally expand or sort our cultures while maintaining their capacity to proliferate, we worked with a heterogenous population and assessed the impact of CRISPR-Cas9 at the culture level using
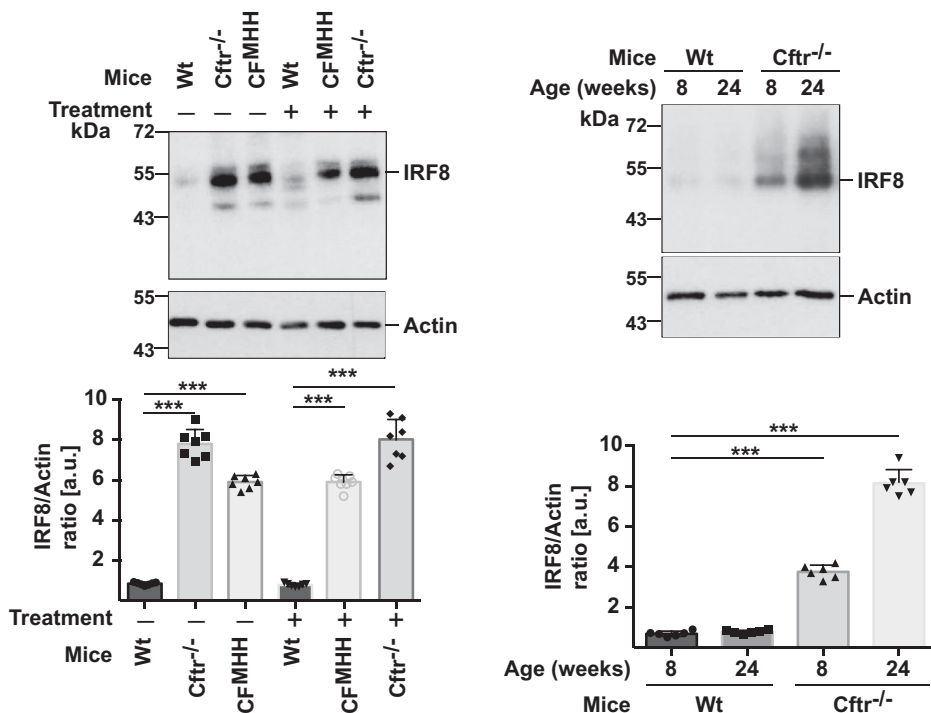
Figure 1. Cftr deficiency induces an upregulation of IRF8—biochemical analysis and a downregulation of acid ceramidase. *Left panel*, trachea from wild-type (Wt) or Cftr-deficient (Cftr$^{-/-}$) or Cftr-deficient mice with a residual activity of Cftr (CF^{MHH}) were removed and incubated for 2 h in H/S in the absence or presence of 10 µg/ml *P. aeruginosa* lipopolysaccharide (LPS). The trachea were then lysed, separated on 7.5% SDS-PAGE, blotted, and analyzed for IRF8 expression. Actin served as loading controls to confirm similar amounts of protein in each lane. *Right panel*, trachea from 8-week (young) and 24-week (old) wild-type or Cftr$^{-/-}$ mice were removed, immediately lysed, and analyzed as above. All western blots were quantified and normalized to actin expression. Shown are representative blots and the mean ± SD of the quantitative analysis from six independent experiments; ***$p < 0.001$, ANOVA and post hoc *t*-test.

both the GeneArt Genomic Cleavage Detection Kit and at the protein level *via* Western blotting.

Transfection of epithelial cells with CRISPR/Cas9 constructs targeting the IRF8 gene resulted in reduction of IRF8 mRNA in cells from CF individuals by 69 ± 2.2%. IRF8 mRNA reduction translated in a marked reduction and even normalization of IRF8 protein levels in epithelial cells from CF individuals (Fig. 5B) and an increase of acid ceramidase activity (Fig. 5C) in these cells. Ceramide was increased in CF epithelial cells compared with cells from healthy individuals and normalized by genetically targeting IRF8 (Fig. 5D).

Next, we transfected Caco-2 cells with siRNA targeting IRF8 to suppress expression of IRF8 or with control siRNA. Transfection of IRF8-targeting siRNA resulted in an upregulation of acid ceramidase activity in Caco-2 cells (Fig. 6A), a reduction of ceramide levels (Fig. 6B), and an increase of cellular sphingosine (Fig. 6C). Control western blots confirm the downregulation of IRF8 upon siRNA transfection (Fig. 6D). Control siRNA was without effect on expression levels of IRF8 (Fig. 6D). More importantly, transfection of siRNA targeting IRF8 prevented downregulation of acid ceramidase expression, increase of ceramide, and downregulation of sphingosine levels upon treatment with the CFTR Inhibitor-172 indicating that CFTR deficiency regulates the acid ceramidase/ceramide/sphingosine system *via* IRF8 (Fig. 6, A–C).

To gain some insight into the mechanisms mediating the increase of IRF8 expression in CF cells, we treated freshly isolated trachea from wild-type and CF mice with the proteasomal inhibitor Mg-132 and tested whether the inhibitor increases expression of IRF8 in wild-type epithelial cell and further increases expression of IRF8 in CF cells. However, the inhibitor did not influence protein expression of IRF8 in wild-type or in CF cells (not shown). Next, we tested whether forced overexpression of the acid ceramidase has an impact on IRF8 expression employing mice overexpressing the acid ceramidase as a transgene and lacking Cftr. The results show that overexpression of acid ceramidase partially normalized the expression of IRF8 in Cftr-deficient bronchial epithelial cells (Fig. 7, A and B).

In order to show the functional significance of the IRF8-mediated regulation of cellular acid ceramidase expression and sphingosine levels, we transfected Caco-2 cells with siRNA targeting IRF8 to suppress IRF8 (Fig. 7C) or with control siRNA. The cells were then treated with the CFTR Inhibitor-172 or left untreated. We then infected the cells with *P. aeruginosa* for 2 h at a multiplicity of infection of 0.1. Untransfected or control transfected Caco-2 cells reduced the number of *P. aeruginosa* in the cultures (Fig. 7C) indicating a cell immanent antibacterial mechanism. This reduction of bacterial numbers was prevented by addition of anti-sphingosine antibodies indicating that it was mediated by sphingosine. Suppression of IRF8 increased resistance of untreated cells to *P. aeruginosa* slightly (Fig. 7C). Treatment of Caco-2 cells with CFTR Inhibitor-172 reduced the resistance
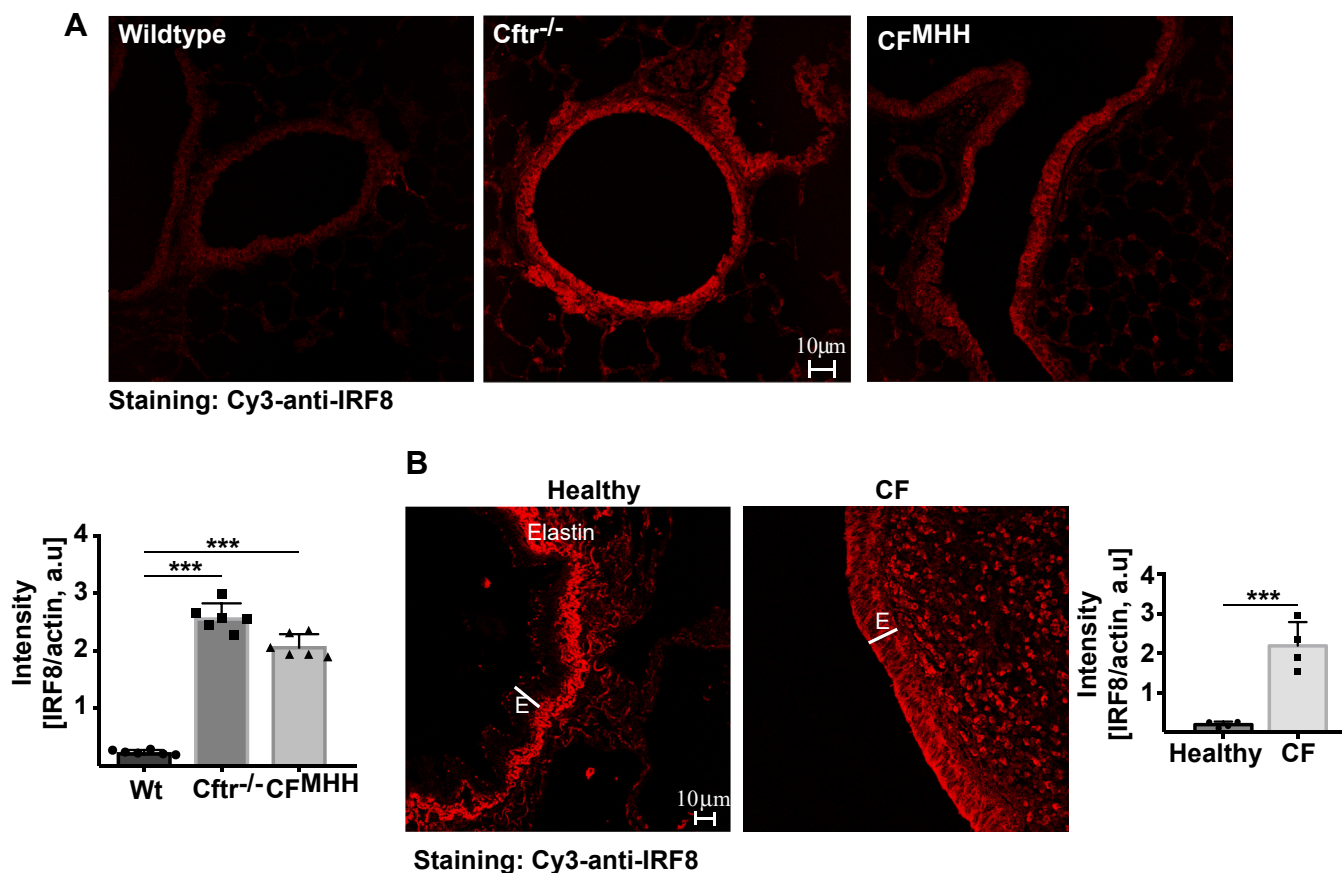
Figure 2. Cftr/CFTR deficiency induces an upregulation of IRF8—immunofluorescence confocal microscopy. *A*, trachea from 24-week-old wild-type (Wt) or Cftr$^{-/-}$ or CF^{MHH} mice were removed, fixed in 4% PFA, embedded, sectioned, dewaxed, and immunostained with Cy3-coupled anti-IRF8 antibodies. All figures were made with the same settings of the confocal microscopy. Fluorescence intensity was quantified using Photoshop. IRF8 expression was normalized to actin fluorescence in epithelial cells. Shown are representative immunostainings and the mean ± SD of the quantitative analysis from six each independent samples; ***$p < 0.001$, ANOVA and post hoc *t*-test. *B*, sections from explanted lungs from CF patients and from donor lungs were immunostained for IRF8 and analyzed by confocal microscopy. Shown are representative results from six CF lungs and three healthy controls. Fluorescence intensity was quantified using Photoshop and IRF8 expression was normalized to actin fluorescence in epithelial cells. The mean ± SD of the quantitative analysis is given; ***$p < 0.001$, ANOVA and post hoc *t*-test. E, epithelial cell layer. Please note that the strong signal under the epithelial cell layer in healthy lungs is caused by the autofluorescence of elastin, which is reduced in fibrotic CF lungs.

of the cells to *P. aeruginosa* and increased the survival of the bacteria (Fig. 7*C*). Resistance of CFTR Inhibitor-172-treated cells was restored by downregulation of IRF8 upon transfection of siRNA targeting IRF8 in cells incubated with the CFTR Inhibitor-172-treated cells (Fig. 7*C*). Incubation of CFTR Inhibitor-172-treated cells with ceramidase or sphingosine also normalized the resistance of the cells to the pathogen (Fig. 7*C*). The resistance of these cells to the infection was again reverted by addition of anti-sphingosine antibodies during the infection (Fig. 7*C*).

Discussion

In the present article, we demonstrate that genetic deficiency or pharmacological inhibition of CFTR/Cftr results in an upregulation of IRF8 mRNA and protein in human and murine CF tracheal and bronchial epithelial cells. The upregulation of IRF8 results in downregulation of the acid ceramidase as evidenced by the observation that suppression of IRF8 expression by CRISPR/Cas9 technology prevented downregulation of acid ceramidase in primary human CF

bronchial epithelial cells. In accordance, suppression of IRF8 expression in Caco-2 epithelial cells using siRNA technology also prevented the downregulation of acid ceramidase in these cells upon treatment with the CFTR Inhibitor-172.

The IRF8-mediated downregulation of acid ceramidase in CF cells resulted in accumulation of ceramide and downregulation of cellular sphingosine levels. The imbalance of the two lipids was corrected in CFTR Inhibitor-172-treated cells by genetic downregulation of IRF8 supporting a key role of IRF8 for the regulation of sphingolipid metabolism in CF cells. Likewise, the accumulation of ceramide in fully differentiated cultured human tracheal epithelial cells was also corrected by suppression of IRF8 expression. Collectively, these data provide genetic proof for a link between CFTR/Cftr, upregulation of IRF8 in CFTR/Cftr-deficient cells and downregulation of the acid ceramidase.

Expression levels of IRF8 increased with age of the CF mice consistent with the previous finding that older CF mice (age of 16 weeks and older) have a higher infection susceptibility than young CF mice (6) and also consistent with the finding that the symptoms of CF progressively develop with age.
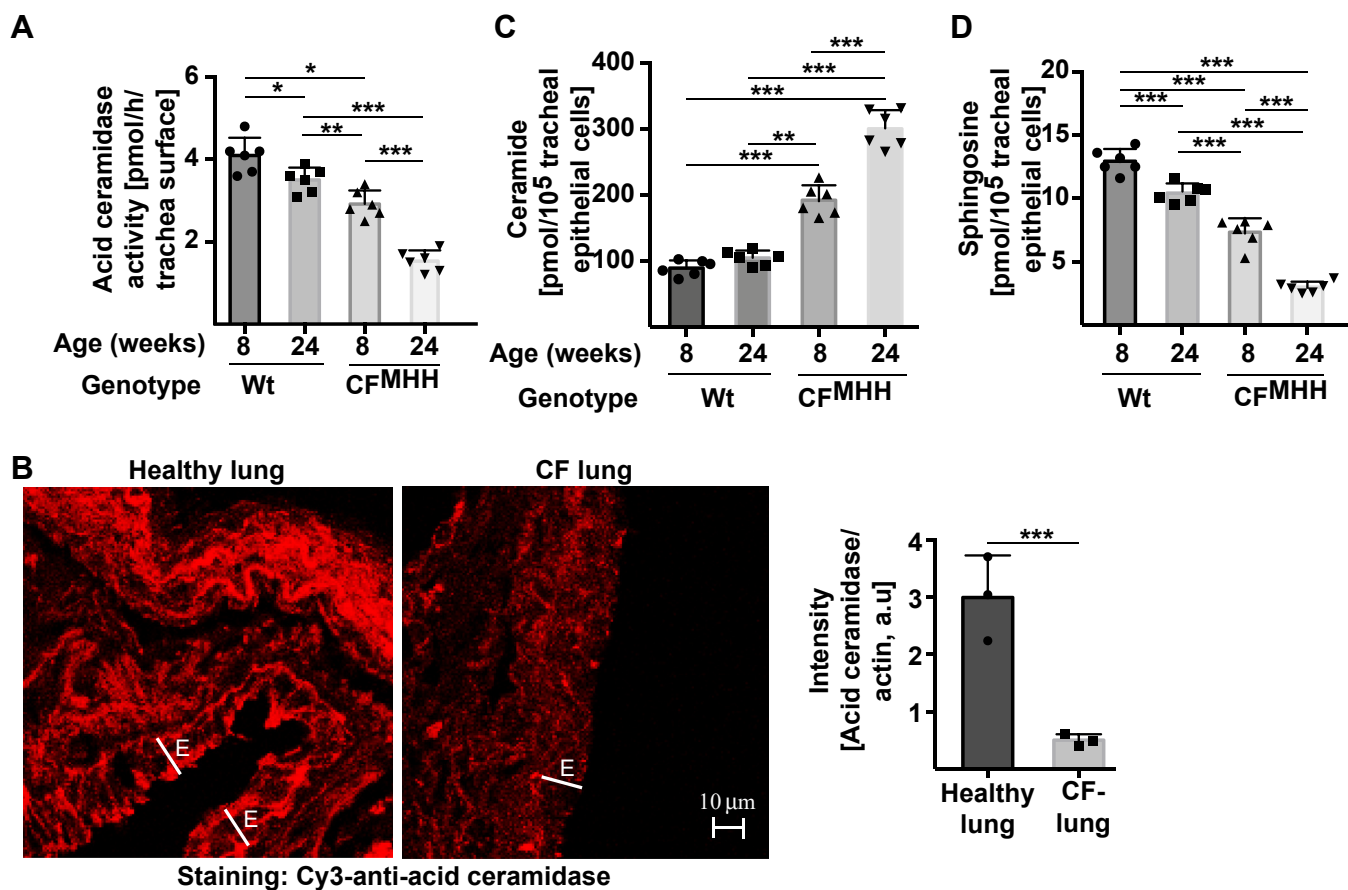
Figure 3. Cftr/CFTR deficiency induces a downregulation of acid ceramidase, which correlates with increased ceramide and decreased sphingosine levels in tracheal epithelial cells from CF mice. *A*, acid ceramidase activity in the epithelial cell layer from wild-type (Wt) and CF^{MHH} mice was determined by incubation of the cell surface with [^{14}C]C$_{16}$ceramide and measuring of its consumption to sphingosine and the fatty acid. Given are the mean ± SD of the acid ceramidase activities from each of the six independent samples; *$p < 0.05$, **$p < 0.01$, ***$p < 0.001$, ANOVA and post hoc *t*-test. *B*, sections from explanted lungs from CF patients and from donor lungs were immunostained for acid ceramidase and analyzed by confocal microscopy. Shown are representative results from six CF lungs and three healthy controls. Fluorescence intensity was quantified as above and normalized to actin fluorescence in epithelial cells. The mean ± SD of the quantitative analysis is shown; ***$p < 0.001$, ANOVA and post hoc *t*-test. E, epithelial cell layer. Ceramide (*C*) and sphingosine (*D*) in young (8 weeks) and old (24 weeks) wild-type (Wt) and CF^{MHH} were determined in isolated tracheal epithelial cells by kinase assays. Given are the total amounts of ceramide and sphingosine. Shown are the mean ± SD from six independent experiments; **$p < 0.01$, ***$p < 0.001$, ANOVA and post hoc *t*-test.

A previous study on human chronic myelogenous leukemia cells has shown that IRF8 is a repressor of acid ceramidase expression in leukemic cells (26), consistent with the present findings. These studies also demonstrated that IRF8 directly binds to the promoter region of the acid ceramidase gene (*ASAH1*). Likewise, IRF8-deficient mice showed a marked overexpression of the acid ceramidase in myeloid cells (26), further supporting the notion that IRF8 represses the expression of the acid ceramidase.

Our studies are also consistent with a previous report on transcriptome profiling in CF cells that showed an upregulation of IRF1, IRF2, IRF8, and STAT2 transcription factor activity (27).

Our data support the notion that CFTR/Cftr functions as a repressor of IRF8 expression and deficiency or functional inhibition of CFTR/Cftr results in upregulation of IRF8. At present it is unknown how CFTR/Cftr-deficiency results in an upregulation of IRF8. It remains to be determined whether alterations in ubiquitination and/or proteolytic degradation of IRF8, autophagy, or lysosomal functions in CF cells result in the accumulation of IRF8 (28–30) or whether CFTR/Cftr controls the expression of IRF8 by regulating its transcription. Our data showing that the mRNA and protein levels for IRF8 are markedly increased in fully differentiated human tracheal epithelial cells suggests that CFTR/Cftr regulates IRF8 transcription. On the other hand, it has been previously shown that ubiquitination regulates IRF8 degradation in activated macrophages (28). However, proteolysis is not impaired in CF cells, and consistent with our data employing a proteasome inhibitor, it is unlikely that the expression of IRF8 is increased by a defect in the proteasome.

It might be possible that deficiency of CFTR/Cftr results in an alkalization of lysosomes (6, 30) and thereby in a functional imbalance of the acid ceramidase and the acid sphingomyelinase activities within lysosomes and a subsequent initial accumulation of ceramide in lysosomes. In addition, it was shown that ceramide synthesis is upregulated in CF cells and might also cause or contribute, respectively, to an initial
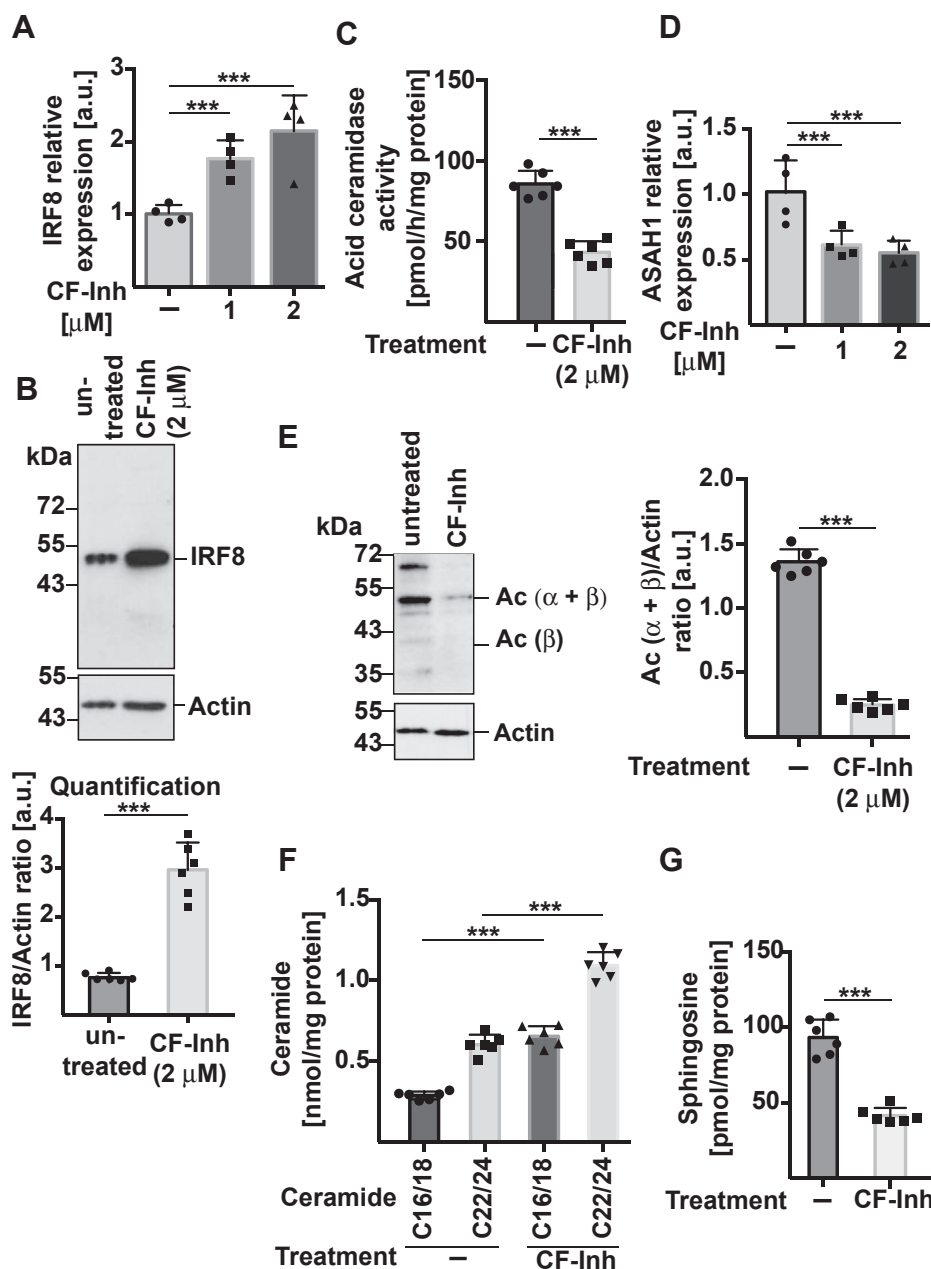
Figure 4. Pharmacological inhibition of CFTR upregulates IRF8 and downregulates acid ceramidase. *A* and *B*, Caco-2 epithelial cells were treated with the pharmacological CFTR Inhibitor-172 (CF-Inh, 1 or 2 µM) for 2 days or left untreated, lysed, and expression of IRF8 was determined by quantitative PCR (*A*) or western blotting (*B*). To determine activity (*C*) and expression (*D* and *E*) of the acid ceramidase Caco-2 epithelial cells were treated with the CFTR Inhibitor-172 for 2 days or left untreated, and lysed. *C*, acid ceramidase activity was measured by consumption of [^{14}C]C$_{16}$ceramide. Expression of acid ceramidase mRNA (*D*) and protein (*E*) (Ac, α and β subunit) was analyzed by quantitative PCR or western blotting. Ceramide (*F*) and sphingosine (*G*) levels were analyzed in Caco-2 epithelial cells by kinase assays upon treatment with the CFTR Inhibitor-172 for 2 days. Given are the total amounts of ceramide and sphingosine. Western blots in panel *B* and *E* were quantified and normalized to actin expression. Shown are representative blots (*B* and *E*) and the mean ± SD of the quantitative studies from each of the six (*B*, *C*, *E*, *F* and *G*) or four (*A* and *D*) independent experiments; ***$p < 0.001$, ANOVA and post hoc *t*-test.

increase of ceramide (15, 17, 31). This initial rise of ceramide might trigger, *via* unknown mechanisms, the upregulation of IRF8, which then results in a physical downregulation of acid ceramidase expression and thereby in further accumulation of ceramide and depletion of sphingosine, finally resulting in a vicious cycle in CF cells. This model is supported by our data indicating that forced (transgenic) overexpression of the acid ceramidase in Cftr-deficient mice normalizes the expression levels of IRF8.

The Jak/Stat pathway, which is activated by interferons, has been previously shown to stimulate expression of IRF proteins (32). However, Stat activity has been shown to be reduced in CF cells due to an increase in expression of protein inhibitor of activated Stat1 (33). Thus, it seems to be unlikely that the increased expression of IRF8 is caused by a constitutive activation of Jak/Stat pathways in CF cells.

The molecular mechanisms mediating the age-dependent upregulation of IRF8 in CF cells also remain to be
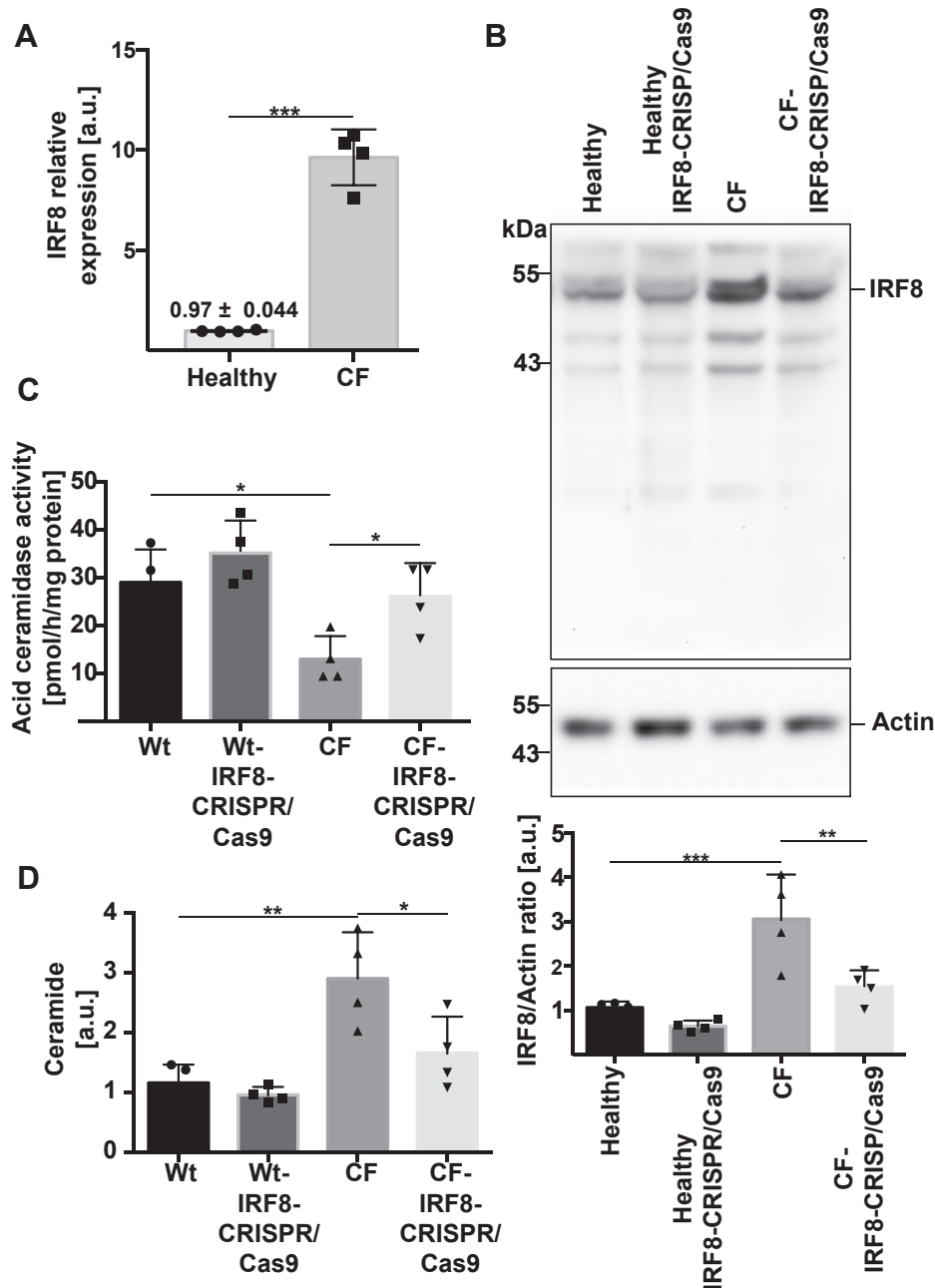
Figure 5. CFTR deficiency in differentiated human epithelial cells induces a downregulation of acid ceramidase *via* an upregulation of IRF8. IRF8-mRNA (*A*), IRF8 protein levels (*B*), and acid ceramidase activities (*C*) were determined by western blotting and enzyme activity assay in cultures of human airway epithelial cells from healthy and CF individuals. To target IRF8 expression, cells were transfected with CRISPR/Cas9 constructs targeting the IRF8 gene (IRF8-CRSPR/Cas9). The density of the IRF8 and acid ceramidase signals in the western blots were quantified using band densitometry. Ceramide levels (*D*) were determined in untransfected or IRF8-targeted human epithelial cells by a fluorescent activity assay and dot blotting of lipid fractions. The SD is very small in panel *A*, and we gave the numerical value for easier identification. Shown are mean ± SD of the quantitative studies from each of the four independent experiments; *$p < 0.05$, **$p < 0.01$, ***$p < 0.001$, ANOVA and post hoc *t*-test.

determined, but this observation is consistent with the age-dependent bacterial colonization of the lungs of children with CF.

The present data also support the notion that sphingosine plays a central role in the cellular defense against *P. aeruginosa*, since the reconstitution of sphingosine in CFTR Inhibitor-172-treated cells upon (i) suppression of IRF8 or (ii) generation of sphingosine employing a neutral ceramidase or

(iii) supplementation of sphingosine restored the defense of these cells against *P. aeruginosa*.

In summary, we identify that IRF8 is a major regulator of the altered sphingolipid metabolism in CF cells. Increased ceramide and decreased sphingosine levels cause the infection susceptibility of CF mice. Thus, a targeted suppression of IRF8 expression in CF cells might be a novel approach to prevent infections in CF mice.
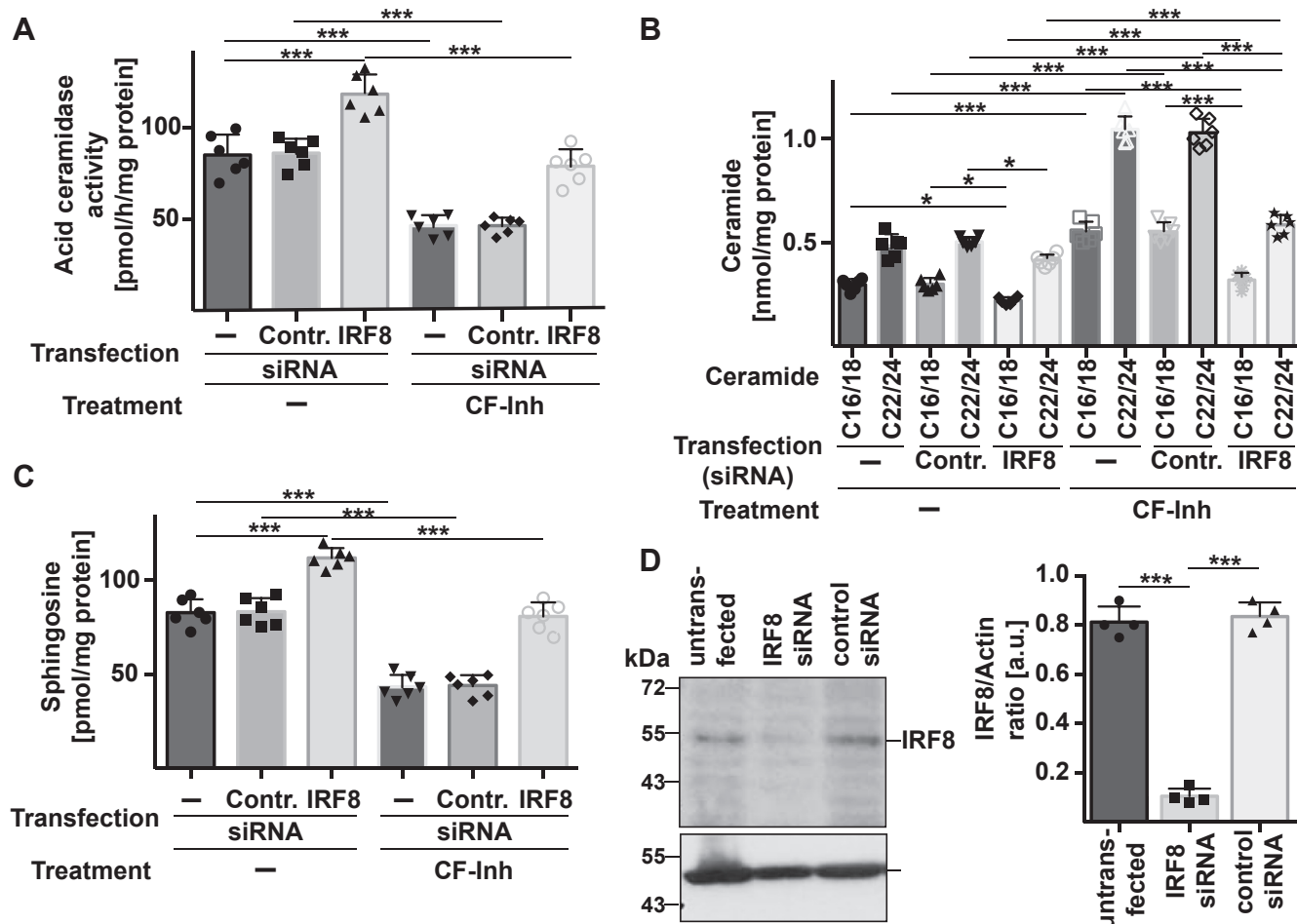
Figure 6. Modification of IRF8 expression regulates acid ceramidase expression. SiRNA-mediated suppression of IRF8 expression results in upregulation of acid ceramidase activity (*A*), downregulation of ceramide (*B*), and upregulation of sphingosine (*C*) in Caco-2 cells expression, while control siRNA has no effect on acid ceramidase, ceramide, and sphingosine (*A–C*). Treatment with the CFTR Inhibitor-172 (CF-Inh, 2 μM) results in an IRF8-dependent downregulation of acid ceramidase activity, an increase of ceramide, and a downregulation of sphingosine, events that are prevented by suppression of IRF8 expression, but not by control (contr.) siRNA. Cells were transiently transfected with siRNA targeting IRF8 or control siRNA by electroporation. Cells were analyzed 48 h after transfection. Cells were left untreated or treated for 2 days with 2 μM CFTR Inhibitor-172. Cells were then lysed and the activity of acid ceramidase and the concentrations of ceramide and sphingosine were determined as above. Expression of IRF8 after transfection of siRNA targeting IRF8 or control siRNA was controlled by western blotting (*D*). Actin served as loading control. Blots were quantified and normalized to actin. Given are the total amounts of ceramide and sphingosine. Shown are the mean ± SD or representative blots from six independent experiments; *$p < 0.05$, ***$p < 0.001$, ANOVA and post hoc *t*-test.

Experimental procedures

Human lung sections

Tissue sections were obtained from explanted CF or remaining donor lungs. Tissue biopsies were fixed in 4% paraformaldehyde (PFA) for 48 h and then embedded in paraffin. The studies were approved by the local ethics committees Essen under the permission numbers 17-7326-BO. All experiments followed the Declaration of Helsinki principles.

Human epithelial cells

Primary human bronchial epithelial cells from young people with and without CF were isolated and cultured to confluent monolayers as previously described (34). Informed consent was obtained for sampling (UK National Research Ethics Committee reference 15/NE/0215), also following the Declaration of Helsinki principles. Cells from four individual donors were used in each group (CF group was all homozygous for the *F508del CFTR* mutation, non-CF group all negative on newborn screening for CF and sampled at the time of a clinically indicated bronchoscopy).

Mice

B6.129P2(CF/3)-*Cftr*[TgH(neoim)Hgu] (CF[MHH]) congenic mice were generated by inbreeding the original *Cftr*TgH[(neoim)]Hgu mutant mouse, which was obtained by insertional mutagenesis in exon 10 of the Cftr gene (35, 36). This congenic *CF[MHH]* strain was backcrossed for more than 20 generations into the B6 background. Because these mice still express low levels of Cftr, they can be fed a standard mouse diet. *CF[MHH]* mice exhibit normal development, but also display pulmonary pathology typical of CF (6, 10, 11, 14, 37). Syngenic B6 littermates were used as controls.

We also used *Cftr*[tm1Unc]-*Tg*[(FABPCFTR)] mice (*Cftr*^{−/−}; Jackson Laboratory) backcrossed for more than ten generations onto
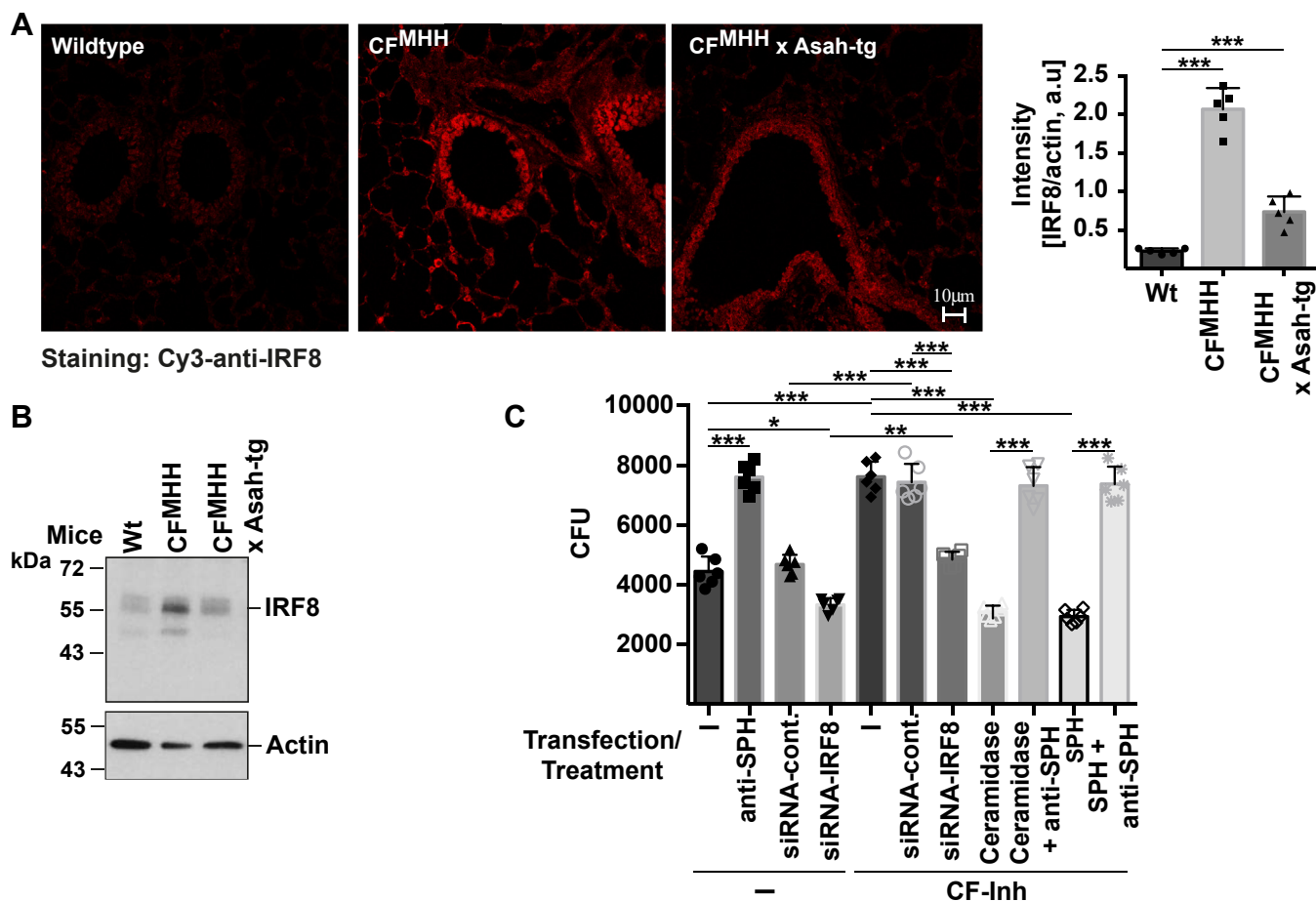
Figure 7. Mechanisms of IRF8 upregulation in CF cells, which regulates the cellular defense against *P. aeruginosa* via sphingosine. *A*, trachea from wild-type, CF, and and CFxAsah-tg mice were isolated, fixed in 4% paraformaldehyde, embedded in paraplast, sections were performed and stained with Cy3-coupled anti-IRF8 antibodies. The fluorescence signals were quantified and normalized to the fluorescence signal obtained in the epithelial cells for staining with FITC-phalloidin. *B*, in addition, proteins were extracted and western blots for IRF8 expression were performed. Shown are representative confocal microscopy studies and blots and the mean ± SD of the quantitative analysis from five independent experiments; ***$p < 0.001$, ANOVA and post hoc *t*-test. *C*, Caco-2 cells were transiently transfected with siRNA targeting IRF8 or control siRNA and treated with the CFTR Inhibitor-172 (CF-Inh, 2 μM) for 2 days or left untreated. Cells were then infected with *P. aeruginosa* at a multiplicity of infection (MOI) of 0.1 and the number of the bacteria after 2 h incubation was determined. Surface sphingosine was neutralized by addition of 1 μg/ml anti-sphingosine antibodies added 15 min prior to the infection. Sphingosine on the cell surface was increased by addition of sphingosine (1 μM) or purified neutral ceramidase (1 μg/ml) 15 min prior to infection. Shown are the mean ± SD of the bacterial numbers in the cultures measured as colony forming units (CFU) from six independent experiments; *$p < 0.05$, **$p < 0.01$, ***$p < 0.001$, ANOVA and post hoc *t*-test.

the C57BL/6 background. These mice are deficient in *Cftr* in all organs except the intestine, where they express human CFTR under the control of a FABP promoter. The transgene prevents intestinal obstruction and allows the mice to have a normal diet. Syngenic B6 littermates were used as controls. We did not notice important differences between the *Cftr⁻/⁻* and the *CF^MHH* strains in the present experiments.

CF^MHH mice were crossed with mice transgenic for Asah1 to achieve overexpression of the acid ceramidase in mice lacking Cftr (19). Asah1 transgenic mice were also on a C57BL/6 background. Overexpression of the acid ceramidase was achieved by introducing an expression cassette in which Asah1 is expressed under control of the CAG promoter into the mouse genome. Mice were cloned and integration of the transgene was tested by PCR. Overexpression of the acid ceramidase was confirmed by measuring acid ceramidase activity in several tissues.

In the present studies we used female and male mice with an age of at least 16 weeks and a weight between 25 and 35 g. Mice were divided into cages of equal size (usually 3–4 mice) by animal unit technical staff with no involvement in study design. Cages were randomly assigned to an experimental group. The investigators were blinded to the group allocation during the experiment and/or when assessing the outcome.

Mice were housed and bred within isolated cages in the mouse facility of the University Hospital, University of Duisburg-Essen, Germany. They were repeatedly tested for a panel of common murine pathogens according to the 2002 recommendations of the Federation of European Laboratory Animal Science Associations. The mice were free of all pathogens. Animal procedures were approved by the Bezirksregierung Duesseldorf, Duesseldorf, Germany, under the number 81-02.04.2019.A134.

Targeting IRF8 in human epithelial cells

Cells were grown until ∼50% confluent in a 6-well plate format. CRISPR-Cas9-mediated downregulation was performed using a validated TrueGuide Synthetic sgRNA (#A35533, Thermo Fisher, 37.5 pmol per well) targeting *IRF8* and TrueCut Cas9 Protein v2 (#A36496, Thermo Fisher, 6 µg per well) was delivered *via* Lipofectamine CRISPRMAX Cas9 Transfection reagent (#CMAX00001, Thermo Fisher, 7.5 µl) per manufacturer's protocol for A549 cells. Cells were allowed to recover for 24 h before passage for downstream applications. As we were unable to clonally expand or apply cell sorting technologies to our primary cultures, we utilized heterogeneous cultures containing both positive and negative cells. To assess the overall impact of this approach at the culture level, a small fraction of each culture was analyzed using the GeneArt Genomic Cleavage Detection Kit (#A24372, Thermo Fisher) per manufacturer's instructions to assess culture downregulation efficiency. This was also validated at the protein level *via* western blotting.

Real-time qPCR on cell extracts

Cultures of human epithelial cells were scraped into 1 ml of ice-cold PBS before being pelleted at 5000*g*. Samples were then processed as per the Purelink RNA Micro Kit manufacturer's instructions (#12183016, Thermo Fisher). RNA concentration and quality were determined using a NanoDrop One (Thermo-Fisher). Standard concentrations of cDNA were generated using random hexamer primers. Relative gene expression was determined by real-time qPCR. One nanogram of previously standardized cDNA per sample (in duplicate) was analyzed using the primers and conditions described on a QuantStudio 3 system (Thermo Fisher). "Template only" and "negative only" controls were performed as required, and genes of interest were normalized against combined *GAPDH, ACTB,* and *TUBB*. Data are presented as fold change ($2^{-\Delta\Delta Ct}$) relative to untreated non-CF samples. Primers were for IRF8: Forward: AGGTCTTCGA-CACCAGCCAGTT, Reverse: GCACGAGAATGAGTTTG GAGCG; for ASAH1: Forward: ACCAGTGCCTGGCCTACTT, Reverse: AACAGCGGCAATACCCTTCA; for GAPDH: Forward: GTCTCCTCTGACTTCAA, Reverse: ACCACCCTGTT GCTGTA; for ACTB: Forward: TGAGAGGGAAATCGTGCG TG, Reverse: TGCTTGCTGATCCACATCTGC;

for TUBB: Forward: ACTACCAGCCACCCTCTGTGTC, Reverse: GCACAAACGCACGATTACA.

Caco-2 cells were treated for 48 h with 1 or 2 µM CFTR Inhibitor-172 or left untreated. Total RNA of Caco-2 cells was isolated using the RNeasy Mini Kit (Qiagen) according to the manufacture's instructions. RNA concentration and quality were determined using a NanoDrop One (Thermo Fisher). cDNA was generated using the RNA-to-cDNA reverse transcription kit (Promega, #A5000). Relative gene expression (in triplicate) was performed on a QuantStudio 5 system (Thermo Fisher). The relative mRNA abundance was calculated using the 2-ΔΔCt method. Gene expression data was normalized to ACTB and GAPDH. Primers were as above.

Western blots

Human epithelial cells

Cultures were scraped into 1 ml of ice-cold 0.1% SDS, 25 mM HEPES, 0.5% deoxycholate, 0.1% Triton X-100, 10 mM EDTA, 10 mM sodium pyrophosphate, 10 mM NaF, 125 mM NaCl (RIPA buffer) containing a protease inhibitor cocktail (Roche). Samples were vortexed for 30 s before being briefly sonicated. Protein concentration was determined by BCA protein assay and samples were stored at –80 °C prior to analysis. In total, 20 µg of whole cell lysates was separated by sodium dodecyl sulfate–polyacrylamide gel electrophoresis (SDS-PAGE) and transferred to PVDF membranes (BioRad). Membranes were blocked for 1 h with 3% BSA in PBST (Sigma) before being probed with primary rabbit anti-IRF8 (1:1000; Cell Signaling, #5628) or anti-acid ceramidase antibodies (1:100; Mybiosource, MBS1492517) and isotype-matched HRP-conjugated secondary antibodies (1:10,000; Thermo Fisher, #31460). Membranes were then treated with SuperSignal West PICO plus chemiluminescent substrate (Pierce) and exposed to film. Membranes were stripped and reprobed for β-actin.

Murine tissue samples and Caco2 cells

Trachea from wild-type or CF mice were removed, briefly washed in H/S, and immediately lysed in 25 mM HEPES, 3% NP40, 0.1% Triton X-100, 10 mM EDTA, 10 mM sodium pyrophosphate, 10 mM sodium fluoride, 125 mM NaCl, and 10 µg/ml aprotinin/leupeptin. If the trachea were treated with *P. aeruginosa* lipopolysaccharide (LPS, Sigma, #L9143), they were treated with 10 µg/ml LPS or left untreated for 2 h in H/ S, then washed and lysed as above. Trachea were also treated for 4 h with 10 µM Mg-132 (Abcam, #141003) prior to lysis and analysis. Caco-2 cells were treated with 2 µM CFTR Inhibitor-172 for 48 h or left untreated, washed in H/S, and also lysed as above. Samples were lysed for 5 min at 4 °C, centrifuged at 14,000 rpm for 5 min at 4 °C, the supernatants were added to 5x SDS-Laemmli buffer, boiled, and proteins were separated by 8.5% or 10% SDS-PAGE for the analysis of IRF8 or acid ceramidase expression, respectively. The gels were blotted onto nitrocellulose membranes overnight, blocked in Starting Block Tris-buffered saline (TBS) blocking buffer (Thermo Fisher Scientific, #37542) for 60 min, washed and incubated for 60 min with anti-IRF8 antibodies or antiacid ceramidase antibodies. All antibodies were diluted 1:1000-fold in Starting Block (TBS) blocking buffer (Pierce, #37542). Blots were washed five times in TBS/0.05% Tween, incubated for 60 min with alkaline phosphatase (AP)-coupled anti-rabbit antibodies (1:50,000, Abcam, #ab97048) or AP-coupled anti-mouse antibodies (1:50,000, Abcam, #ab97020), washed again five times in TBS/0.05% Tween, washed twice in alkaline wash buffer, and developed with the CDP-STAR with NitroBlockII Enhancer system (PerkinElmer). As controls, we blotted and blocked aliquots of the samples as above and incubated the blots with HRP-coupled anti-actin antibodies (1:200,000, Santa Cruz Inc, #sc47778) for 60 min. Blots were washed as above and developed.

Acid ceramidase activity

Human epithelial cells

A derivation of the previously described fluorescent ceramidase and sphingomyelinase assays was utilized to determine enzyme activity ([16]). Briefly, cultures were lysed in 1% Nonidet P40 (NP40) in 150 mM sodium acetate (pH 4.5), kept for 5 min on ice, and diluted to a standard total protein concentration of 1 mg/ml in NP40 in 150 mM sodium acetate (pH 4.5). In total, 200 µl of each culture lysate was incubated with 100 nmol of BODIPYTR ceramide (#D7540, Thermo Fisher) at 37 °C for 30 min. The reaction was terminated and separated and analyzed on a Typhoon fluorescence plate reader.

Murine tissue samples and Caco2 cells

The trachea was removed, carefully opened, and the surface of the epithelial cell layer was incubated with 4 µl $[^{14}C_{16}]$ceramide (55 mCi/mmol, #ARC-0831, ARC) for 20 min $[^{14}C_{16}]$ ceramide was dried, resuspended in 0.05% octylglucopyranoside in 150 mM sodium acetate (pH 7.4 or 5.0), and bath sonicated for 10 min prior to addition to the trachea. The trachea was then extracted in H_2O and $CHCl_3:CH_3OH:HCl$ (100:100:1, v/v/v). Caco-2 cells were lysed in 1% Nonidet P40 (NP40) in 150 mM sodium acetate (pH 4.5) for 5 min on ice, diluted to 0.1% NP40 in 150 mM sodium acetate (pH 4.5), and 0.3 µCi/sample $[^{14}C_{16}]$ceramide (ARC0831, 55 mCi/mmol) was added as above. The samples were incubated at 37 °C for 60 min. The reaction was terminated by extraction in H_2O and $CHCl_3:CH_3OH:HCl$ (100:100:1, v/v/v). The lower phase was dried, and samples were resuspended in $CHCl_3:CH_3OH$ (1:1, v/v), separated by thin-layer chromatography (TLC) with $CHCl_3:CH_3OH:NH_4OH$ (90:20:0.5, v/v/v), and analyzed with a Fuji Imager.

Immunohistochemistry of human and mouse lungs

Stainings were performed as previously reported ([6], [7], [9], [38], [39]). For immunohistochemical evaluation of murine lungs, mice were sacrificed by cervical dislocation, immediately perfused *via* the right heart with ice-cold normal saline for 2 min followed by cardiac perfusion with 4% PBS-buffered PFA (#0335.3, Roth) for 10 to 15 min. The lungs were removed and further fixed in 4% PFA for 36 to 40 h, serially dehydrated with an Ethanol to Xylol gradient, embedded in paraffin, sectioned at 7 µm, dewaxed, and rehydrated. Human lung tissues were fixed in 4% PFA/PBS for 48 h followed by dehydration, sectioning, and rehydration as for the mouse tissue.

To retrieve antigens, the samples were incubated with pepsin (Digest All; #003009, Invitrogen) for 30 min at 37 °C, washed with water and PBS, and unspecific antibody binding sites were blocked for 10 min at room temperature with PBS, 0.05% Tween 20 (Sigma), and 5% fetal calf serum (FCS). The samples were stained with mouse monoclonal anti-IRF8 antibodies (1:200 dilution; Santa Cruz Inc, #365042) or rabbit anti-

acid ceramidase antibodies (1:200; ProSci, #4741) in H/S (132 mM NaCl, 20 mM HEPES [pH 7.4], 5 mM KCl, 1 mM $CaCl_2$, 0.7 mM $MgCl_2$, 0.8 mM $MgSO_4$) plus 1% FCS at room temperature for 45 min. Samples were washed three times with PBS plus 0.05% Tween 20, once with PBS, were incubated for 45 min with Cy3-coupled anti-rabbit $F(ab)_2$ fragments (1:500; Jackson Immunoresearch, #711-166-152) or Cy3-coupled anti-mouse $F(ab)_2$ fragments (1:500; Jackson Immunoresearch, #711-166-150) in H/S plus 1% FCS for secondary fluorescence labeling. The samples were again washed three times with PBS plus 0.05% Tween 20 and once with PBS. Samples were then stained with FITC-phalloidin (1:1000, Sigma, #P5282). Samples were washed again and finally embedded in Mowiol. Samples were evaluated by confocal microscopy using a Leica TCS-SL confocal microscope equipped with a 40× lens, and images were analyzed with Leica LCS software version 2.61 (Leica Microsystems). All comparative samples were measured at identical settings.

All immunostainings were controlled with isotype control antibodies that showed no or very weak staining. These were purified mouse IgG for anti-IRF8 stainings and rabbit IgG for the stainings with antiacid ceramidase (Dako). We also included controls with secondary Cy3-coupled antibodies only. These controls confirmed the specificity of the stainings and revealed no significant background stainings.

Caco-2 cells and CFTR Inhibitor-172 treatment

The CFTR Inhibitor-172 (Sigma, #C2992) was dissolved in DMSO at 10 mM stock concentration. It was then diluted into cell culture medium to incubate Caco-2 cells with the inhibitor at 1 µM or 2 µM. Controls were incubated with the same concentration of DMSO.

Caco-2 cells were grown in MEM medium supplemented with 10 mM HEPES (pH 7.4; Carl Roth GmbH), 2 mM L-glutamine, 1 mM sodium pyruvate, 100 µM nonessential amino acids, 100 U/ml penicillin, 100 µg/ml streptomycin (all from Invitrogen), and 10% FCS (PAA Laboratories GmbH).

Sphingosine and neutral ceramidase

Sphingosine (Avanti Polar Lipids, #860490P) was resuspended as a 20 mM stock solution in 0.9% NaCl, sonicated to obtain a suspension and promote the formation of micelles, and stored at –20 °C. Sphingosine was bath sonicated (Bandelin Sonorex) for 10 min prior any experiment. The same volume of 0.9% NaCl as used was added to all control samples. Neutral ceramidase (R&D, #3557-AH-010, specific activity: 5000 pmol/min/µg) was used as provided. Cells were incubated with 10 µM sphingosine for 15 min or 1 µg/ml neutral ceramidase for 30 min, washed with H/S, and infected with *P. aeruginosa*.

Sphingosine kinase assay

Epithelial cells were removed from the trachea by carefully scraping the inner surface of the trachea and were extracted in

200 µl H$_2$O and 800 µl CHCl$_3$:CH$_3$OH:1N HCl (100:200:1, v/v/v). Caco-2 cells were treated with 2 µM CFTR-Inhibitor-172 or left untreated for 2 days. In addition, Caco-2 cells were transfected with siRNA targeting IRF8 or control-siRNA. Cells were also lysed in 200 µl H$_2$O and 800 µl CHCl$_3$:CH$_3$OH:1N HCl (100:200:1, v/v/v). Phases were separated, the lower phase was dried and resuspended in a detergent solution (7.5% [w/v] n-octyl glucopyranoside, 5 mM cardiolipin in 1 mM diethylenetriaminepentaacetic acid [DTPA]). The kinase reaction was initiated by addition of 0.001 units sphingosine kinase (R&D, #6068-SK-010) in 50 mM HEPES (pH 7.4), 250 mM NaCl, 30 mM MgCl$_2$ 1 mM ATP and 10 µCi [^{32}P]γATP. Samples were incubated for 60 min at 37 °C at 350 rpm and then extracted by addition of 100 µl H$_2$O, 20 µl 1N HCl, 800 µl CHCl$_3$:CH$_3$OH:1N HCl (100:200:1, v/v/v), and 240 µl each of CHCl$_3$ and 2 M KCl. Phases were separated, the lower phase was collected, dried, dissolved in 20 µl CHCl$_3$:CH$_3$OH (1:1, v/v), and separated on Silica G60 TLC plates with CHCl$_3$:CH$_3$OH:acetic acid:H$_2$O (90:90:15:5, v/v/v/v) as developing solvent. The TLC plates were analyzed with a phosphorimager. Sphingosine levels were determined with a standard curve of C18-sphingosine.

Ceramide kinase assays

Caco-2 cells or tracheal epithelial cells were prepared as above and lysed in 200 µl H$_2$O, the lysates were extracted in CHCl$_3$:CH$_3$OH:1N HCl (100:100:1, v/v/v), and phases were separated by 5 min at 14,000 rpm centrifugation of the samples. The lower phase was collected, dried, and resuspended in 20 µl of a detergent solution (7.5% [w/v] n-octyl glucopyranoside, 5 mM cardiolipin in 1 mM diethylenetriaminepentaacetic acid [DTPA]). The samples were sonicated for 10 min in a bath sonicator to promote the formation of micelles. The kinase reaction was initiated by adding 70 µl of a reaction mixture containing 10 µl diacylglycerol (DAG) kinase (GE Healthcare Europe), 0.1 M imidazole/HCl (pH 6.6), 0.2 mM DTPA (pH 6.6), 70 mM NaCl, 17 mM MgCl$_2$, 1.4 mM ethylene glycol tetraacetic acid, 2 mM dithiothreitol, 1 µM adenosine triphosphate (ATP), and 5 µCi [^{32}P]γATP (6000 Ci/mmol; Hartmann Radiochemicals). The kinase reaction was performed for 60 min at room temperature with 300 rpm shaking. Samples were then organically extracted in 1 ml CHCl$_3$:CH$_3$OH:1N HCl (100:100:1, v/v/v), 170 µl buffered saline solution (135 mM NaCl, 1.5 mM CaCl$_2$, 0.5 mM MgCl$_2$, 5.6 mM glucose, 10 mM HEPES [pH 7.2]), and 30 µl of a 100 mM EDTA solution was added, and the phases were separated. The lower phase was collected, dried in a SpeedVac, separated on Silica G60 TLC plates with chloroform/acetone/methanol/acetic acid/H$_2$O (50:20:15:10:5, v/v/v/v/v), and developed with a Fuji phosphoimager. Ceramide amounts were determined by comparison with a standard curve using C16–C24 ceramides as substrates.

Ceramide in humans was also determined by a dot blot method. To this end, cultures were scraped into 500 µl ice-cold PBS and agitated to disperse cell clumps. In total, 10 µl was removed for BCA protein assay (Pierce) and the remainder pelleted at 5000g. Samples were resuspended in varying volumes of deionized water to a standard concentration of 1 µg/ml. In total, 2 µl of each sample was then dotted onto a PVDF membrane (BioRad) and allowed to air dry. Membranes were then blocked, probed, and visualized with the primary mouse anti-ceramide (1:500, Glycobiotech, MAB_0010) and appropriate isotype-matched HRP-conjugated secondary antibodies.

Downregulation of IRF8 in Caco-2 cells

The expression of IRF8 in Caco-2 cells was downregulated by transfection with commercial siRNA targeting IRF8 (Santa Cruz Inc; # sc35630). Control, irrelevant siRNA was also from Santa Cruz Inc (# sc37007). Cells were transiently transfected by electroporation at 400 V with 5 pulses, 3 ms each, with a BTX electroporator. Dead cells were removed after 24 h, and cells were cultured for an additional 24 h before analysis of acid ceramidase expression, ceramide and sphingosine levels. Downregulation of IRF8 was confirmed by western blotting as described above.

P. aeruginosa infections

P. aeruginosa strain American Type Culture Collection (ATCC) 27853, a laboratory strain, was grown overnight on tryptic soy agar (TSA; Becton Dickinson Biosciences), transferred to tryptic soy broth (TSB, Becton Dickinson Biosciences) at a density of an OD$_{550nm}$ of 0.2 to 0.25, and the bacteria were grown for 1 h at 37 °C with 125 rpm shaking to reach the early logarithmic phase in order to obtain reproducible growth conditions. Bacteria were then centrifuged at 1710g for 10 min, washed once in sterile HEPES/Saline (H/S; 132 mM NaCl, 20 mM HEPES [pH 7.4], 5 mM KCl, 1 mM CaCl$_2$, 0.7 mM MgCl$_2$, 0.8 mM MgSO$_4$), resuspended in H/S, and added to the cells at a multiplicity of infection (MOI) of 0.2 bacteria: 1 cell.

Cells were either left untreated prior to the infection or treated with 5 µM CFTR-Inhibitor-172 for 24 h. CFTR-Inhibitor-172-treated cells were either infected without further treatment or sphingosine was reconstituted in these cells by incubation for 15 min with 1 µM sphingosine. In addition, we transfected Caco-2 cells with siRNA-targeting IRF8 or control siRNA and used them for the infection experiments.

Quantification and statistical analysis

All data are expressed as arithmetic means ± SD. For the comparison of continuous variables from independent groups, we used one-way ANOVA followed by post hoc Student's t-tests for all pairwise comparisons and the Bonferroni correction for multiple testing. The p values for the pairwise comparisons were calculated after Bonferroni correction. All values were normally distributed. Statistical significance was set at the level of $p \leq 0.05$ (two-tailed). Sample size planning for the continuous variable was based on two-sided Wilcoxon–Mann–Whitney tests (free software: G*Power Version 3.1.7, University of Duesseldorf, Germany). Blots and fluorescence stainings were quantified using Photoshop. Investigators were blinded to the identity of the samples in all microscopy experiments.

Data availability

All data are available on request from the authors. Authors confirm that all data are included in the article.

References

1. Riordan, J. R., Rommens, J. M., Kerem, B., Alon, N., Rozmahel, R., Grzelczak, Z., Zielenski, J., Lok, S., Plavsic, N., Chou, J. L., Drumm, M. L., Iannuzzi, M. C., Collins, F. S., and Tsui, L. C. (1989) Identification of the cystic fibrosis gene: Cloning and characterization of complementary DNA. *Science* **245**, 1066–1073
2. Kerem, B., Rommens, J. M., Buchanan, J. A., Markiewicz, D., Cox, T. K., Chakravarti, A., Buchwald, M., and Tsui, L. C. (1989) Identification of the cystic fibrosis gene: Genetic analysis. *Science* **245**, 1073–1080
3. Elborn, J. S. (2016) Cystic fibrosis. *Lancet* **388**, 2519–2531
4. Bhagirath, A. Y., Li, Y., Somayajula, D., Dadashi, M., Badr, S., and Duan, K. (2016) Cystic fibrosis lung environment and *Pseudomonas aeruginosa* infection. *BMC Pulm. Med.* **16**, 174
5. CF Foundation (2019) *Patient Registry Annual Report*, Cystic Fibrosis Foundation, Bethesda, MD
6. Teichgräber, V., Ulrich, M., Endlich, N., Riethmüller, J., Wilker, B., De Oliveira-Mundin, C. C., van Heeckeren, A. M., Barr, M. L., von Kürthy, G., Schmid, K. W., Weller, M., Tümmler, B., Lang, F., Grassmé, H., Döring, G., *et al.* (2008) Ceramide accumulation mediates inflammation, cell death and infection susceptibility in cystic fibrosis. *Nat. Med.* **14**, 382–391
7. Pewzner-Jung, Y., Tavakoli Tabazavareh, S., Grassmé, H., Becker, K. A., Japtok, L., Steinmann, J., Joseph, T., Lang, S., Tuemmler, B., Schuchman, E. H., Lentsch, A. B., Kleuser, B., Edwards, M. J., Futerman, A. H., and Gulbins, E. (2014) Sphingoid long chain bases prevent lung infection by *Pseudomonas aeruginosa*. *EMBO Mol. Med.* **6**, 1205–1214
8. Tavakoli Tabazavareh, S., Seitz, A., Jernigan, P., Sehl, C., Keitsch, S., Lang, S., Kahl, B. C., Edwards, E., Grassmé, H., Gulbins, E., and Becker, K. A. (2016) Lack of sphingosine causes susceptibility to pulmonary *Staphylococcus aureus* infections in cystic fibrosis. *Cell. Physiol. Biochem.* **38**, 2094–2102
9. Grassmé, H., Henry, B., Ziobro, R., Becker, K. A., Riethmüller, J., Gardner, A., Seitz, A. P., Steinmann, J., Lang, S., Ward, C., Schuchman, E. H., Caldwell, C. C., Kamler, M., Edwards, M. J., Brodlie, M., *et al.* (2017) β1-Integrin accumulates in cystic fibrosis luminal airway epithelial membranes and decreases sphingosine, promoting bacterial infections. *Cell Host Microbe* **21**, 707–718
10. Becker, K. A., Riethmüller, J., Lüth, A., Döring, G., Kleuser, B., and Gulbins, E. (2010) Acid sphingomyelinase inhibitors normalize pulmonary ceramide and inflammation in cystic fibrosis. *Am. J. Respir. Cell Mol. Biol.* **42**, 716–724
11. Becker, K. A., Henry, B., Ziobro, R., Tümmler, B., Gulbins, E., and Grassmé, H. (2012) Role of CD95 in pulmonary inflammation and infection in cystic fibrosis. *J. Mol. Med. (Berl.)* **90**, 1011–1023
12. Bodas, M., Min, T., Mazur, S., and Vij, N. (2011) Critical modifier role of membrane-cystic fibrosis transmembrane conductance regulator-dependent ceramide signaling in lung injury and emphysema. *J. Immunol.* **186**, 602–613
13. Brodlie, M., McKean, M. C., Johnson, G. E., Gray, J., Fisher, A. J., Corris, P. A., Lordan, J. L., and Ward, C. (2010) Ceramide is increased in the lower airway epithelium of people with advanced cystic fibrosis lung disease. *Am. J. Respir. Crit. Care Med.* **182**, 369–375
14. Ulrich, M., Worlitzsch, D., Viglio, S., Siegmann, N., Iadarola, P., Shute, J. K., Geiser, M., Pier, G. B., Friedel, G., Barr, M. L., Schuster, A., Meyer, K. C., Ratjen, F., Bjarnsholt, T., Gulbins, E., *et al.* (2010) Alveolar inflammation in cystic fibrosis. *J. Cyst. Fibros.* **9**, 217–227
15. Caretti, A., Bragonzi, A., Facchini, M., De Fino, I., Riva, C., Gasco, P., Musicanti, C., Casas, J., Fabriàs, G., Ghidoni, R., and Signorelli, P. (2014) Anti-inflammatory action of lipid nanocarrier-delivered myriocin: Therapeutic potential in cystic fibrosis. *Biochim. Biophys. Acta* **1840**, 586–594
16. Gardner, A. I., Haq, I. J., Simpson, A. J., Becker, K. A., Gallagher, J., Saint-Criq, V., Verdon, B., Mavin, E., Trigg, A., Gray, M. A., Koulman, A., McDonnell, M. J., Fisher, A. J., Kramer, E. L., Clancy, J. P., *et al.* (2020) Recombinant acid ceramidase reduces inflammation and infection in cystic fibrosis. *Am. J. Respir. Crit. Care Med.* **202**, 1133–1145
17. Loberto, N., Mancini, G., Bassi, R., Carsana, E. V., Tamanini, A., Pedemonte, N., Dechecchi, M. C., Sonnino, S., and Aureli, M. (2020) Sphingolipids and plasma membrane hydrolases in human primary bronchial cells during differentiation and their altered patterns in cystic fibrosis. *Glycoconj. J.* **37**, 623–633
18. Liessi, N., Pesce, E., Braccia, C., Bertozzi, S. M., Giraudo, A., Bandiera, T., Pedemonte, N., and Armirotti, A. (2020) Distinctive lipid signatures of bronchial epithelial cells associated with cystic fibrosis drugs, including Trikafta. *JCI Insight* **5**, e138722
19. Becker, K. A., Verhaegh, R., Verhasselt, H. L., Keitsch, S., Soddemann, M., Wilker, B., Wilson, G. C., Buer, J., Ahmad, S. A., Edwards, M. J., and Gulbins, E. (2020) Acid ceramidase rescues cystic fibrosis mice from pulmonary infections. *Infect. Immun.* **89**, e00677-20
20. Azuma, M. M., Balani, P., Boisvert, H., Gil, M., Egashira, K., Yamaguchi, T., Hasturk, H., Duncan, M., Kawai, T., and Movila, A. (2018) Endogenous acid ceramidase protects epithelial cells from *Porphyromonas gingivalis*-induced inflammation *in vitro*. *Biochem. Biophys. Res. Commun.* **495**, 2383–2389
21. Seitz, A. P., Schumacher, F., Baker, J., Soddemann, M., Wilker, B., Caldwell, C. C., Gobble, R. M., Kamler, M., Becker, K. A., Beck, S., Kleuser, B., Edwards, M. J., and Gulbins, E. (2019) Sphingosine-coating of plastic surfaces prevents ventilator-associated pneumonia. *J. Mol. Med. (Berl.)* **97**, 1195–1211
22. Bibel, D. J., Aly, R., and Shinefield, H. R. (1992) Antimicrobial activity of sphingosines. *J. Invest. Dermatol.* **98**, 269–273
23. Fischer, C. L., Walters, K. S., Drake, D. R., Blanchette, D. R., Dawson, D. V., Brogden, K. A., and Wertz, P. W. (2013) Sphingoid bases are taken up by *Escherichia coli* and *Staphylococcus aureus* and induce ultrastructural damage. *Skin Pharmacol. Physiol.* **26**, 36–44
24. Verhaegh, R., Becker, K. A., Edwards, M. J., and Gulbins, E. (2020) Sphingosine kills bacteria by binding to cardiolipin. *J. Biol. Chem.* **295**, 7686–7696

25. Carstens, H., Schumacher, F., Keitsch, S., Kramer, M., Kühn, C., Sehl, C., Soddemann, M., Wilker, B., Herrmann, D., Swaidan, A., Kleuser, B., Verhaegh, R., Hilken, G., Edwards, M. J., Dubicanac, M., *et al.* (2019) Clinical development of sphingosine as anti-bacterial drug: Inhalation of sphingosine in mini pigs has no adverse side effects. *Cell. Physiol. Biochem.* **53**, 1015–1028

26. Hu, X., Yang, D., Zimmerman, M., Liu, F., Yang, J., Kannan, S., Burchert, A., Szulc, Z., Bielawska, A., Ozato, K., Bhalla, K., and Liu, K. (2011) IRF8 regulates acid ceramidase expression to mediate apoptosis and suppresses myelogeneous leukemia. *Cancer Res.* **71**, 2882–2891

27. Kormann, M. S. D., Dewerth, A., Eichner, F., Baskaran, P., Hector, A., Regamey, N., Hartl, D., Handgretinger, R., and Antony, J. S. (2017) Transcriptomic profile of cystic fibrosis patients identifies type I interferon response and ribosomal stalk proteins as potential modifiers of disease severity. *PLoS One* **12**, e0183526

28. Xiong, H., Li, H., Kong, H. J., Chen, Y., Zhao, J., Xiong, S., Huang, B., Gu, H., Mayer, L., Ozato, K., and Unkeless, J. C. (2005) Ubiquitin-dependent degradation of interferon regulatory factor-8 mediated by Cbl down-regulates interleukin-12 expression. *J. Biol. Chem.* **280**, 23531–23539

29. Luciani, A., Villella, V. R., Esposito, S., Brunetti-Pierri, N., Medina, D., Settembre, C., Gavina, M., Pulze, L., Giardino, I., Pettoello-Mantovani, M., D'Apolito, M., Guido, S., Masliah, E., Spencer, B., Quaratino, S., *et al.* (2010) Defective CFTR induces aggresome formation and lung inflammation in cystic fibrosis through ROS-mediated autophagy inhibition. *Nat. Cell Biol.* **12**, 863–875

30. Di, A., Brown, M. E., Deriy, L. V., Li, C., Szeto, F. L., Chen, Y., Huang, P., Tong, J., Naren, A. P., Bindokas, V., Palfrey, H. C., and Nelson, D. J. (2006) CFTR regulates phagosome acidification in macrophages and alters bactericidal activity. *Nat. Cell Biol.* **8**, 933–944

31. Dechecchi, M. C., Nicolis, E., Mazzi, P., Cioffi, F., Bezzerri, V., Lampronti, I., Huang, S., Wiszniewski, L., Gambari, R., Scupoli, M. T., Berton, G., and Cabrini, G. (2011) Modulators of sphingolipid metabolism reduce lung inflammation. *Am. J. Respir. Cell Mol. Biol.* **45**, 825–833

32. Nelson, N., Kanno, Y., Hong, C., Contursi, C., Fujita, T., Fowlkes, B. J., O'Connell, E., Hu-Li, J., Paul, W. E., Jankovic, D., Sher, A. F., Coligan, J. E., Thornton, A., Appella, E., Yang, Y., *et al.* (1996) Expression of IFN regulatory factor family proteins in lymphocytes. Induction of Stat-1 and IFN consensus sequence binding protein expression by T cell activation. *J. Immunol.* **156**, 3711–3720

33. Kreiselmeier, N. E., Kraynack, N. C., Corey, D. A., and Kelley, T. J. (2003) Statin-mediated correction of STAT1 signaling and inducible nitric oxide synthase expression in cystic fibrosis epithelial cells. *Am. J. Physiol. Lung Cell Mol. Physiol.* **285**, L1286–L1295

34. Haq, I. J., Althaus, M., Gardner, A. I., Yeoh, H. Y., Joshi, U., Saint-Criq, V., Verdon, B., Townshend, J., O'Brien, C., Ben-Hamida, M., Thomas, M., Bourke, S., van der Sluijs, P., Braakman, I., Ward, C., *et al.* (2021) Clinical and molecular characterisation of the R751L-CFTR mutation. *Am. J. Physiol. Lung Cell Mol. Physiol.* **320**, L288–L300

35. Charizopoulou, N., Jansen, S., Dorsch, M., Stanke, F., Dorin, J. R., Hedrich, H. J., and Tümmler, B. (2004) Instability of the insertional mutation in CftrTgH(neoim)Hgu cystic fibrosis mouse model. *BMC Genet.* **5**, 6

36. Charizopoulou, N., Wilke, M., Dorsch, M., Bot, A., Jorna, H., Jansen, S., Stanke, F., Hedrich, H. J., de Jonge, H. R., and Tümmler, B. (2006) Spontaneous rescue from cystic fibrosis in a mouse model. *BMC Genet.* **7**, 18

37. Zhang, Y., Li, X., Grassmé, H., Döring, G., and Gulbins, E. (2009) Alterations in ceramide concentration and pH determine the release of reactive oxygen species by Cftr-deficient macrophages on infection. *J. Immunol.* **184**, 5104–5111

38. Grassmé, H., Jekle, A., Riehle, A., Schwarz, H., Berger, J., Sandhoff, K., Kolesnick, R., and Gulbins, E. (2001) CD95 signaling via ceramide-rich membrane rafts. *J. Biol. Chem.* **276**, 20589–20596

39. Grassmé, H., Jendrossek, V., Riehle, A., von Kurthy, G., Berger, J., Schwarz, H., Weller, M., Kolesnick, R., and Gulbins, E. (2003) Host defense against *Pseudomonas aeruginosa* requires ceramide-rich membrane rafts. *Nat. Med.* **9**, 322–330